Available online at www.sciencedirect.com

ScienceDirect

Journal of Catalysis 249 (2007) 289–299

JOURNAL OF CATALYSIS

www.elsevier.com/locate/jcat

Hydrogen production in the decomposition and steam reforming of methanol on Mo_2C/carbon catalysts

Róbert Barthos [a], Frigyes Solymosi [a,b,*]

[a] *Reaction Kinetics Research Group, Chemical Research Centre of the Hungarian Academy of Sciences, University of Szeged, P.O. Box 168, H-6701 Szeged, Hungary*

[b] *Institute of Solid State and Radiochemistry, University of Szeged, P.O. Box 168, H-6701 Szeged, Hungary*

Received 10 March 2007; revised 8 May 2007; accepted 8 May 2007

Abstract

Mo_2C prepared by the reduction and reaction of MoO_3 with carbon Norit and with multiwall carbon nanotube was found to be an effective catalyst for the decomposition of methanol to give H_2 and CO. On 5% Mo_2C/Norit catalyst, complete conversion of methanol was attained at temperatures as low as ~623 K. An important feature of this catalyst is its high thermal stability; the percentages of H_2 (~65%) and CO (24–26%) were practically constant at 573–723 K. The selectivity of hydrogen at 573–723 K was >85%. Formaldehyde also was detected, in amounts decreasing with Mo_2C loading and also with temperature. Other minor products were CH_4 and CO_2. On 5% Mo_2C/Norit, the conversion of methanol and the production of H_2 decreased by only a few percentage points even after 17 h at 723 K. Mo_2C produced on multiwall carbon nanotube also proved active for the decomposition of methanol. Adding water to methanol somewhat decreased the CO content and increased the H_2 content in the products.

Keywords: Hydrogen production; Methanol decomposition; Steam reforming of methanol; Mo_2C catalyst; Carbon Norit support; Multiwall carbon nanotube support

1. Introduction

Significant efforts are underway to find an effective catalytic process for the production of hydrogen with possibly less contamination. One of the oldest known reactions is the water–gas shift reaction [1,2], which, due to the presence of CO cannot be used directly for the production of pure H_2 used in fuel cells. The decomposition of methane free of CO would seem to be an attractive reaction [3–10]. Unfortunately, the deposition of carbon on the catalyst surface blocks this reaction, and the removal of carbon makes this approach to H_2 production too complicated.

Recently, attention has turned to using methanol and ethanol as row materials. Their decomposition and reformation on supported transitional metals are very promising processes. Nonetheless, taking into account the wide application of Pt metals in automobile exhaust catalysis and their high price, efforts are also being made toward replacing them with more effective and less expensive materials.

Recently, we found that Mo_2C combined with ZSM-5 is a very active catalyst and promoter in the aromatization not only of C_1–C_8 hydrocarbons [11–13], but also ethanol [14,15] and methanol [16]. But the direction of the ethanol reaction changed, when carbon was applied as a support. Mo_2C prepared on Norit and multiwall carbon nanotubes (CNTs) was found to be an efficient catalyst for the decomposition of ethanol [17,18]. The remarkable feature of the Mo_2C on both Norit and multiwall CNTs is its very high stability. The conversion of ethanol decreased from ~100% only to ~90% after 75 h at 723 K. Another significant feature is that Mo_2C catalyzes mainly the dehydrogenation of ethanol, promoting rupture of C–H bond, and it is not so active in the cleavage of C–C bond to produce methane and CO. As a result, adding water to ethanol has little effect on product distribution and the formation of hydrogen,

---

[*] Corresponding author. Fax: +36 62 420 678.
E-mail address: fsolym@chem.u-szeged.hu (F. Solymosi).

0021-9517/$ – see front matter © 2007 Published by Elsevier Inc.
doi:10.1016/j.jcat.2007.05.003

although Mo_2C catalyzes both the water–gas shift reaction and methane reforming [19,20].

In the present work, we examined the catalytic effect of Mo_2C on the decomposition and reforming of methanol using the same carbon supports as in the study of the reaction of ethanol. Methanol is probably the best source of hydrogen due to the high hydrogen/carbon ratio and the absence of a C–C bond; consequently, we investigated the steam reforming of methanol on various catalysts [21–45]. The copper-based catalysts seem the most promising, although they have the drawback of poor thermal stability at high temperatures. We know of just one previous report (published as the present paper was being prepared) regarding the application of supported Mo_2C in the steam reforming of methanol [46]. There, it was reported that Mo_2C supported by ZrO_2 and Al_2O_3 is superior to an unsupported catalyst. The yield of hydrogen on 30% Mo_2C/ZrO_2 ranged between 50–55% at 673 K, and slowly decreased only after 10 h.

2. Experimental

2.1. Methods

Catalytic reaction was carried out at 1 atm of pressure in a fixed-bed, continuous-flow reactor consisting of a quartz tube (8 mm i.d.) at a temperature range of 523–723 K [46,47]. The flow rate was generally 40 ml/min. The carrier gas was Ar, which was bubbled through the methanol at 300 K: its content was ∼15%. A ∼0.3-g catalyst sample was used, consisting of small (1–2 mm) fragments. Reaction products were analyzed with two gas chromatographs: an HP 5890 equipped with PORAPAQ Q + S packed column and an HP 4890 equipped with PORAPAQ Q + S and a 30-m-long HP-PLOT Al_2O_3 column. Product analysis was carried out using flame ionization and thermal conductivity detectors. In the study of the reaction of methanol–water mixture of different composition, the reactants were introduced into an evaporator with the help of an infusion pump (Medicor Assistor PCI; flow rate, 1.0 ml liquid/h). The evaporator was the flushed with Ar (flow, 36 ml/min). Methanol or methanol–water containing the Ar flow entered the reactor through an externally heated tube avoiding condensation. Each compound was calibrated separately. In most cases, the conversion of methanol was calculated taking into account the amount consumed; in certain cases, it was also determined based on the H and C contents of the reactant and products.

Hydrogen and different product selectivities were defined as

$$S_{H_2} = \frac{x_{H_2}}{\sum x_i n_i}, \quad S_i = \frac{x_i n_i}{\sum x_i n_i},$$

where x_i and x_{H_2} are the molar fractions of product (i) and H_2, respectively, and n_i is half of the number of hydrogen atoms (in the calculation of S_{H_2}) of the number of carbon atoms (in the calculation of S_i) in each molecule of product (i). The yield of H_2 was calculated in the traditional way (selectivity × conversion). To establish the efficiency of the catalyst in terms of hydrogen production, the percentage of the H_2 formed per hydrogen content of the methanol decomposed also was determined; this value is designated H_2 eff.

Table 1
Some characteristic data for Mo_2C/Norit catalysts

Sample	Surface area (m^2/g)	External surface area (m^2/g)	Micropore Area (m^2/g)	Micropore Volume (ml/g)	CO uptake at 300 K (μmol/g_{cat})
Norit (purified)	859.0	278.5	580.5	0.302	–
1% Mo_2C/Norit	942.7	317.1	625.6	0.326	12.4
5% Mo_2C/Norit	956.0	418.3	537.7	0.281	26.1
10% Mo_2C/Norit	807.7	338.4	469.2	0.246	39.4

FTIR spectra of adsorbed gases were recorded with a Biorad (Digilab Div. FTS 155) instrument with a wave number accuracy of ±4 cm^{-1}. All of the spectra presented herein are difference spectra. The background is the spectrum of the pretreated sample before the adsorption of reactants. Thermal desorption measurements (TPD) were carried out in the catalytic reactor. The Mo_2C/Norit sample was treated with C_2H_5OH/Ar gas mixture at 348 K for 30 min. Then the sample was flushed with Ar for 30 min at 348 K and heated gradually in argon (5 K/min), and the desorbing products were analyzed by gas chromatography. The amount of surface carbonaceous deposit formed in the catalytic experiments was determined by temperature-programmed reaction (TPR). After the catalytic experiment, the sample was flushed with Ar at the reaction temperature and cooled to 300–373 K. The sample was heated at a rate of 5 K/min in H_2 flow, and the hydrocarbons thus formed were analyzed.

Characterization of pure and Mo_2C-containing support was carried out using a Micromeritics Gemini apparatus; the main data are given in Table 1. The dispersion of Mo_2C/Norit was determined on in situ-prepared samples by CO pulses in the reactor after the catalysts were cooled in Ar flow to ∼323 K. XP spectra were obtained with a Kratos XSAM 800 instrument using nonmonochromatic AlK_α radiation ($h\nu = 1486.6$ eV) and a 180° hemispherical analyzer at a base pressure of 1×10^{-9} mbar. Binding energies were referenced to the Fermi level of the forming Mo_2C except at the initial stage of the experiments. For this state, the C 1s binding energy of carbon Norit (285.1 eV) was accepted as the reference.

2.2. Materials

Multiwall CNTs and activated carbon Norit (ROW 0.8-mm pellets) were used as supports. The surface area of CNT is 170 m^2/g, and that of Norit is 859 m^2/g. The preparation and purification of CNTs has been described elsewhere [47]. Carbon Norit was purchased from ALFA AESAR. It was purified by treating it with HCl (∼10%) for 12 h at room temperature. After this treatment, metal impurities were <0.02% as determined by ICP-AES. The starting compound for Mo_2C was MoO_3/C, prepared by impregnation of carbon into solution containing the appropriate amount of ammonium heptamolybdate to yield 1, 5, and 10 wt% of Mo_2C. The dried suspension was calcined in air at 673 K for 3 h. Instead of the carburization of MoO_3, we used a recently developed method [48,49] in which MoO_3 on carbon support was heated in the catalytic reactor in H_2 flow up to 973 K with a temperature ramp of 5 K/min.

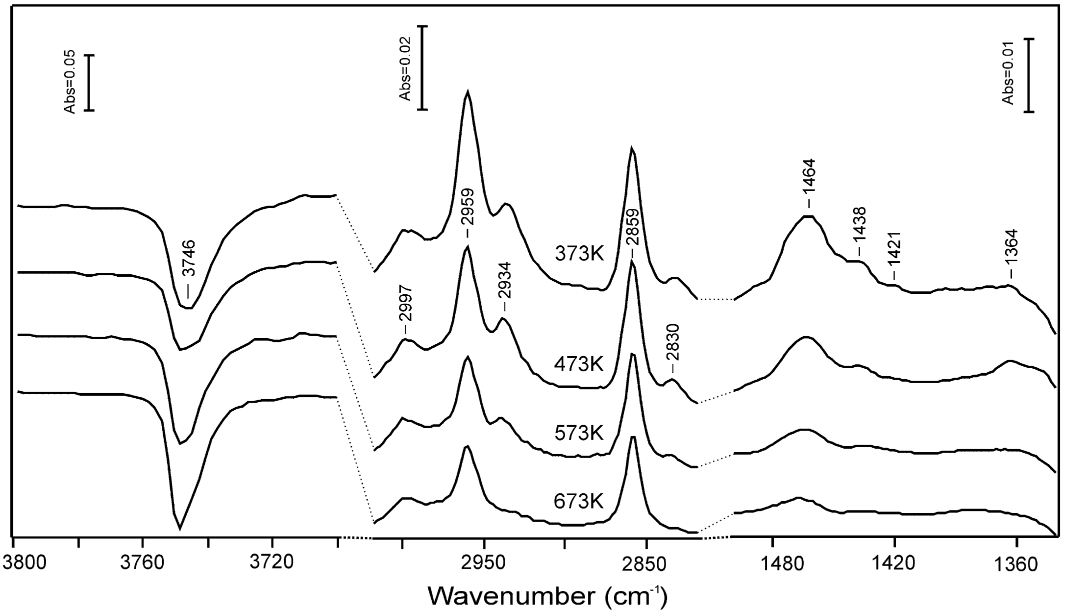

Fig. 1. FTIR spectra following the adsorption of methanol on 5% Mo_2C/SiO_2 at 300 K and after subsequent degassing at different temperatures.

Table 2
Characteristic absorption bands following the adsorption of methanol at 300–373 K

Mode	Gas phase CH_3OH	CH_3OH Mo_2C/ZSM-5 [16]	C_2H_4 Mo_2C/ZSM-5 [16]	CH_3OH $Mo_2C(100)$ [50]	CH_3OH 5% Mo_2C/SiO_2 present study
γ_{OH}	3681				
$\nu_{as}CH_3$	3000	(2996) 2958	2920	2936	(2997) 2957 2934
$\nu_{as}(CH_2)$					
ν_sCH_3	2844	2856	2852		2859, 2830
ν_aCH_2				1441	
$\delta_{as}CH_3$	1477	1472, 1465	1477		1464
δ_sCH_3	1455	1404	1441	1150	1438, 1425
γ_aCH_3			1379		
CH_2-wag (s)					
νCC				1021	
νCO	1033				

XPS measurements reported previously [17,18] demonstrated that Mo_2C formation was complete at 973 K, when the characteristic binding energies of Mo $3d_{3/2}$ and Mo $3d_{5/2}$ of 227.8 and 232.1 eV were attained. Methanol (99.7% purity) was obtained from Spektrum-3D.

3. Results

3.1. Infrared and thermal desorption measurements

Because Mo_2C prepared on Norit is not transparent, we performed FTIR measurements on the 5% Mo_2C/SiO_2 sample. Fig. 1 shows the IR spectra registered after the adsorption of methanol at 300 K for 15 min and subsequent heating of the sample to higher temperature under continuous evacuation. The following spectral changes could be observed at 300 K: a negative feature at 3746 cm^{-1} and the appearance of bands at 2997, 2959, 2934, 2859, 2830, and 1464 cm^{-1} and very weak bands at 1483 and 1421 cm^{-1}. The absorption bands appeared at 300 K, as shown in Table 2, which also presents the characteristic IR features of adsorbed methanol for comparison. The heat treatment of adsorbed layer caused a gradual attenuation of absorption bands without any significant shift in their position. We observed only the development of a weak band at 1940 cm^{-1} above 373 K (not shown in the spectra), which grew with increasing temperature. We found the same features in the presence of 2 or 10% Mo_2C. After annealing the adsorbed layer to 673 K, the weak absorption features at 2934 and 2830 cm^{-1} disappeared.

TPD spectra for various products after adsorption of methanol on 5% Mo_2C/Norit at 323 K are displayed in Fig. 2. The major desorbing products were H_2 ($T_p = 473$ and 748 K) and CH_3OH ($T_p = 398$ K). In addition, the desorption of small amounts of several other compounds—CO and CO_2 ($T_p = 498$ K), methane ($T_p = 498$ and 673 K) and ethane ($T_p = 488$ K)—were measured, and tiny amounts of ethylene were detected above 400 K.

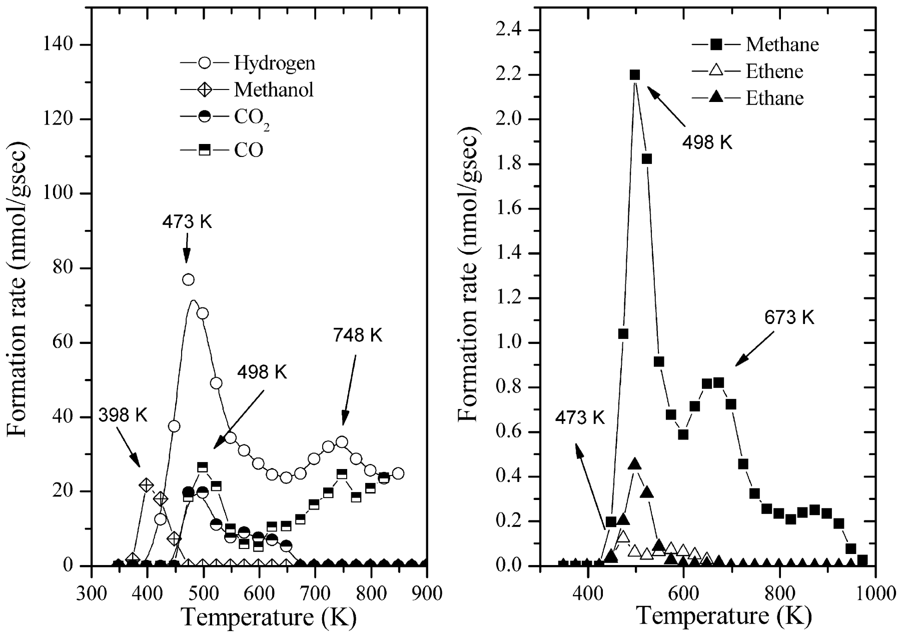

Fig. 2. TPD spectra following ethanol adsorption on 5% Mo_2C/Norit at 300 K.

3.2. Catalytic studies

3.2.1. Decomposition of methanol on Mo_2C/C Norit

The experiments began using the 1% Mo_2C/Norit sample. The decomposition of methanol on this catalyst was noted at above 500 K, and a conversion of ∼80% was attained at ∼773 K. It is important to mention that same conversion values were calculated on the consumption of methanol as well as on the basis of the H and C contents of the methanol introduced and products formed. The rate of evolution of hydrogen increased gradually with increasing temperature, reaching ∼49% at 523 K and 65% at 723 K. The selectivity of H_2 also increased with increasing temperature, reaching a constant value of ∼90% at 723 K. For the C-containing compounds, at lower temperatures (523–573 K), the major product was formaldehyde; its percentage decreased from ∼50% at 523 K to 0 at 723 K. At the same time, CO formation increased gradually, reaching 30% at 723 K. At this temperature the ratio of H_2/CO approached 2. Small amounts of other compounds, including CO_2, CH_4, and C_2–C_3 hydrocarbons, appeared only at and above 573 K. The product distribution as a function of temperature is presented in Fig. 3A.

When the Mo_2C content was increased to 5%, the reaction started at a lower temperature (473 K), and total methanol conversion was achieved at ∼623 K (Fig. 3B). An interesting feature is the disappearance of formaldehyde at 623 K, with selectivity of H_2 exceeding 80% even at 573 K. Only slight changes were observed in the formation of minor products. A further increase in the Mo_2C content to 10% did not lead to a more effective catalyst (Fig. 3C). Moreover, the characteristic data for H_2 and CO formation were somewhat lower compared with those found in previous samples. This was compensated for by the slight increase in the percentages of CO_2 and CH_4. The effect of Mo_2C loading on the product distribution at 573 and 723 K is displayed in Fig. 4. The yields of H_2 production are given in Table 3. As can be seen, around 90% of the hydrogen content of decomposed methanol was converted into gaseous hydrogen on the 1 and 5% Mo_2C/Norit catalysts.

In subsequent experiments, we examined the reaction of methanol in time on stream at 723 K. The results are presented in Fig. 5. The conversion of methanol slowly decayed for 1% Mo_2C/Norit, but remained ∼100% on 5 and 10% Mo_2C/Norit for several hours of reaction. In the case of 5% Mo_2C/Norit, we followed the reaction for 17 h and experienced a slight deterioration of the catalyst only after ∼10 h (Fig. 5B). The percentages and selectivities of H_2 and CO remained practically constant, but the percentages of minor products CH_4 and CO_2 increased slightly (Figs. 5B and 5C).

Results obtained in the study of the space velocity at 623 K are shown in Fig. 6A. In this experiment, the amount of the catalyst was decreased to 100 mg. Under these experimental conditions, the conversion was only ∼58% at the lowest contact time and approached ∼100% at 0.5 $g\,s/cm^3$. The conversion and selectivity of all products except formaldehyde increased with increasing contact time. Analysis of the results presented in Fig. 6B shows that at lower conversion, the production of hydrogen and formaldehyde is favored from 100 moles of converted methanol, while the other products tend to zero. This indicates that the primary reaction is dehydrogenation of methanol to formaldehyde.

3.2.2. Decomposition of methanol on Mo_2C/CNT

It was interesting to see the catalytic behavior of Mo_2C produced on multiwall CNT, which is also effective in the decomposition of ethanol [17,18]. Results, presented in Fig. 7, show the formation of same products as on Mo_2C/Norit samples and very little difference in product distribution. In terms of the minor products, less methane was identified on catalyst containing

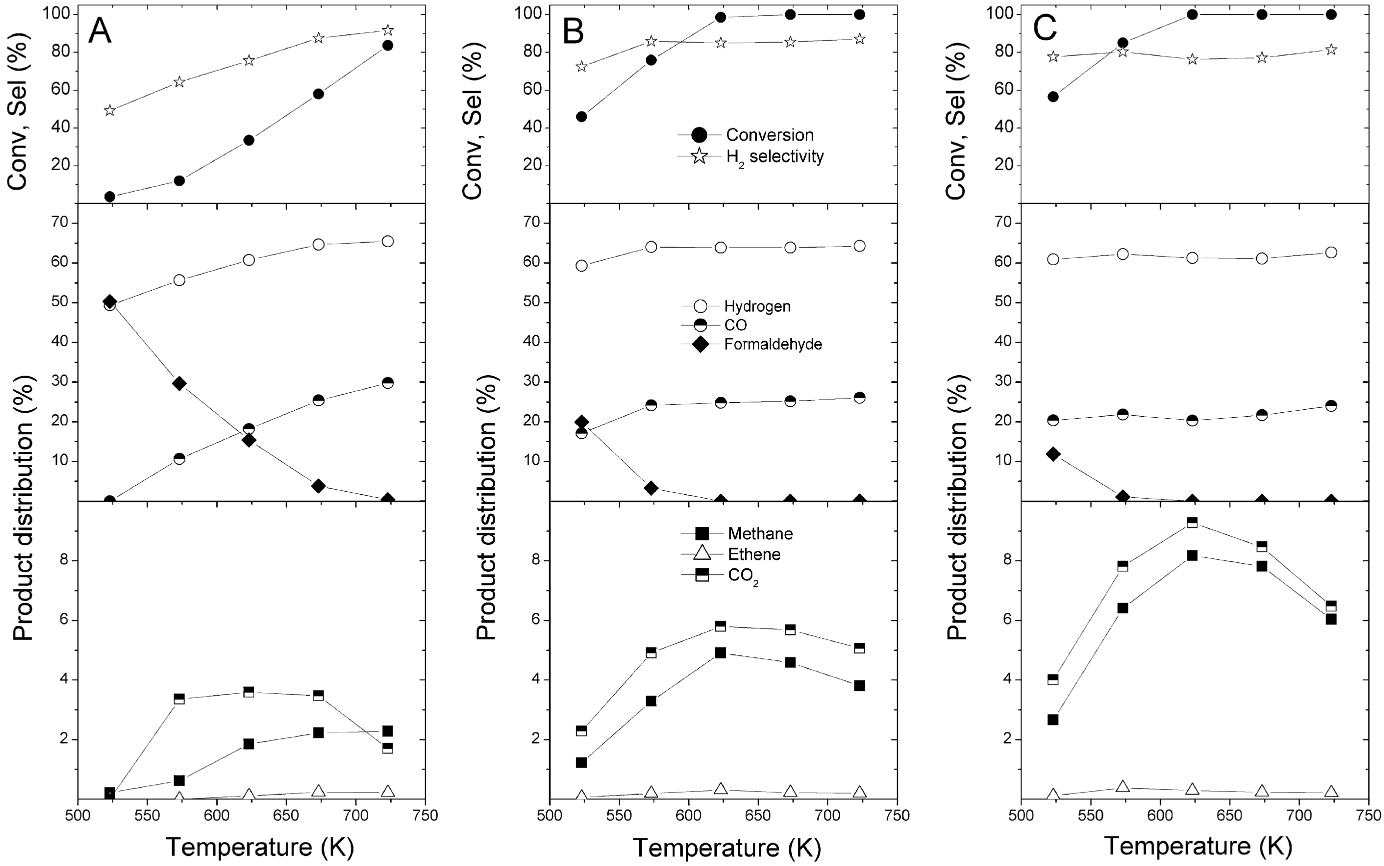

Fig. 3. Reaction of methanol over 1% Mo_2C/Norit (A), 5% Mo_2C/Norit (B), and 10% Mo_2C/Norit (C) at different temperatures. Data were taken at 40 min of the reaction at the given temperature.

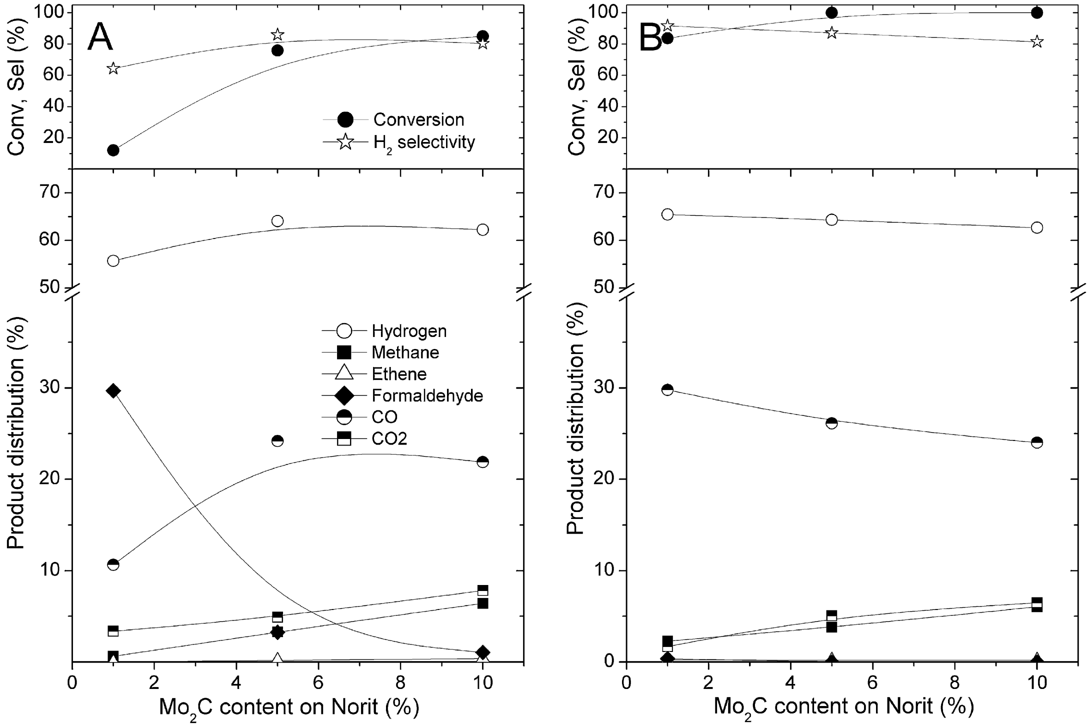

Fig. 4. Effects of Mo_2C content of Norit on the product distribution of the decomposition of methanol at 573 and 723 K. Data were taken at 40 min of the reaction at the given temperature.

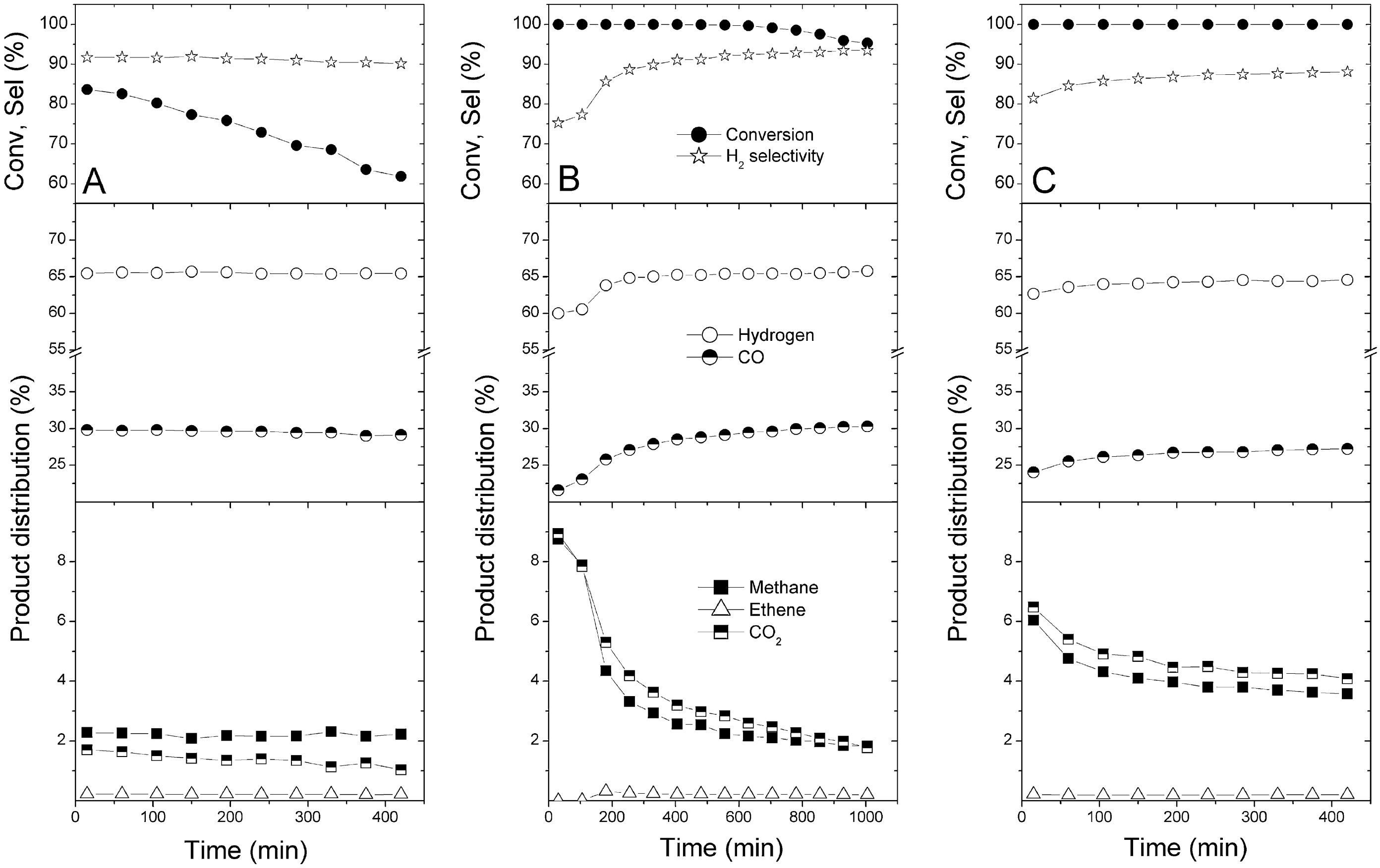

Fig. 5. Reaction of methanol on 1% Mo_2C/Norit (A), 5% Mo_2C/Norit (B), and 10% Mo_2C/Norit (C) in time on stream at 723 K.

Table 3
Yields for the production of H_2 in decomposition and steam reforming of methanol

Catalyst	(A)		(B)	
	623 K	723 K	623 K	723 K
1% Mo_2C/Norit	25.0	72.6	76.4	90.5
5% Mo_2C/Norit	83.8	87.1	88.1	88.9
10% Mo_2C/Norit	76.3	81.5	75.8	80.0
1% Mo_2C/CNT	47.8	52.3	106.3	104.5
5% Mo_2C/CNT	85.2	69.1	95.9	94.5
10% Mo_2C/CNT	91.4	80.8	100.4	99.5

(A) (Selectivity × conversion)/100.
(B) Amount of H_2 formed related to the hydrogen content of methanol decomposed.

10% Mo_2C. In contrast to the Mo_2C/Norit catalyst, deactivation occurred with time on stream at 723 K (Fig. 7C). The product distribution remained practically the same, however.

3.2.3. *Examination of used catalysts*

Our study of the interaction of ethanol with Mo_2C/Norit catalyst in a small reactor attached to the XPS system found an intensification in the weak O 1s signal at 530.4 eV above 623 K [18]. A similar, but somewhat lower, enhancement in the binding energy of O 1s was also seen in the course of methanol decomposition. But, as the catalytic studies show, this change exerted no apparent influence on the behavior of the Mo_2C catalyst.

After completion of the reaction of methanol on 5% Mo_2C/Norit at 723 K for 17 h, we carried out temperature-programmed reaction (TPR) with H_2. The results, plotted in Fig. 8, show that the evolution of methane, ethane, propane and ethylene in decreasing amounts started above 600–650 K with different peak temperatures. The formation of C_2 and C_3 compounds occurred at lower temperatures ($T_p = 773$ and 798 K), and that of methane at higher temperatures ($T_p = 848$ and 1023 K). Another interesting feature is the large amount of methane released. Note that the blank experiment with the unused catalysts also produced some hydrocarbons (albeit more than two orders of magnitude less).

3.3. *Reaction of $CH_3OH + H_2O$ on Mo_2C/Norit*

Detailed experiments were carried out concerning the effect of water on the reaction pathway of methanol on 5% Mo_2C/Norit catalyst. The addition of water to methanol ($H_2O/CH_3OH = 1$) markedly affected the course of the reaction. The total conversion shifted slightly to higher temperatures (673–723 K), and the product distribution underwent even more significant changes (Fig. 9A). Whereas CO was the other major product in the absence of H_2O, in the presence of water, CO_2 formation became prominent. This occurred primarily in the low-temperature range (up to 623 K). Raising the temperature caused a relative increase in the rate of CO and CH_4 formation compared with H_2 and CO_2 formation. Apart from this,

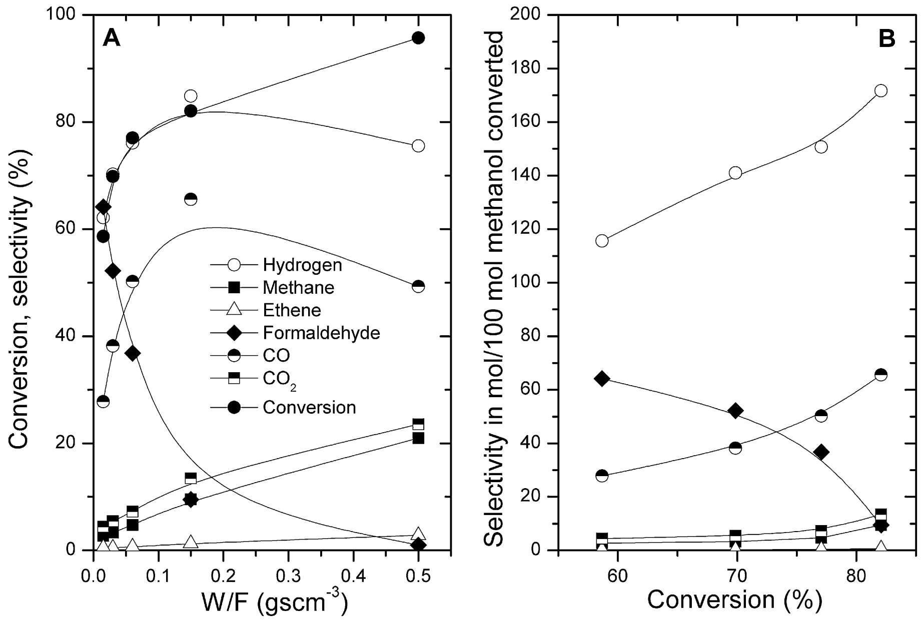

Fig. 6. Effects of space velocity on the product distribution over 5% Mo_2C/Norit (A) and product selectivity as a function of the methanol conversion (B) at 723 K.

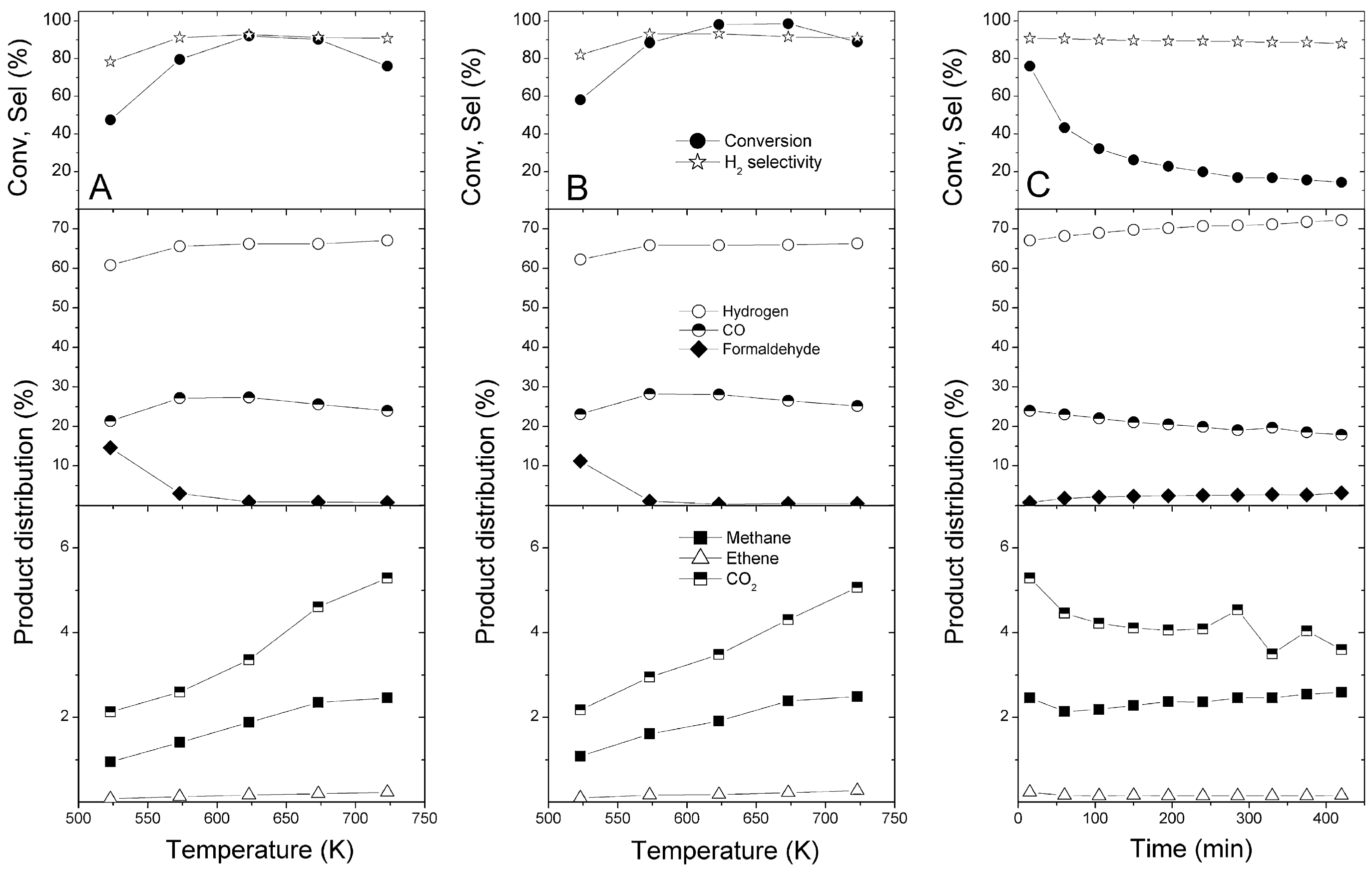

Fig. 7. Reaction of methanol over 1% Mo_2C/CNT (A) and 10% Mo_2C/CNT (B) at different temperatures and in time on stream on 5% Mo_2C/CNT at 723 K (C). Data were taken at 40 min of the reaction at the given temperature.

whereas the percentage of CO was 25% at 623 K (when total conversion was attained [Fig. 3B]), it was reduced to ~8.5% in the presence of water (Fig. 9A). As minor products, ethylene, ethane, propene and butene were formed at <0.5%. When the H_2O/CH_3OH ration was increased to 3, the above-described features remained practically unaltered. Similar features were observed for 10% Mo_2C/Norit, which was initially somewhat more active than the previous sample but slightly less effective

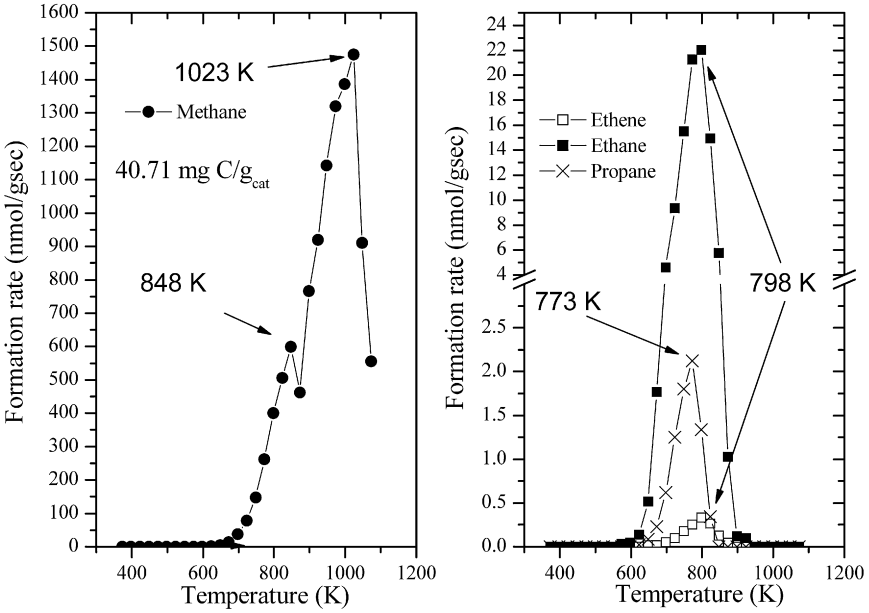

Fig. 8. Formation of hydrocarbons in the TPR measurements following the reaction of methanol on 5% Mo_2C/Norit at 723 K for 17 h.

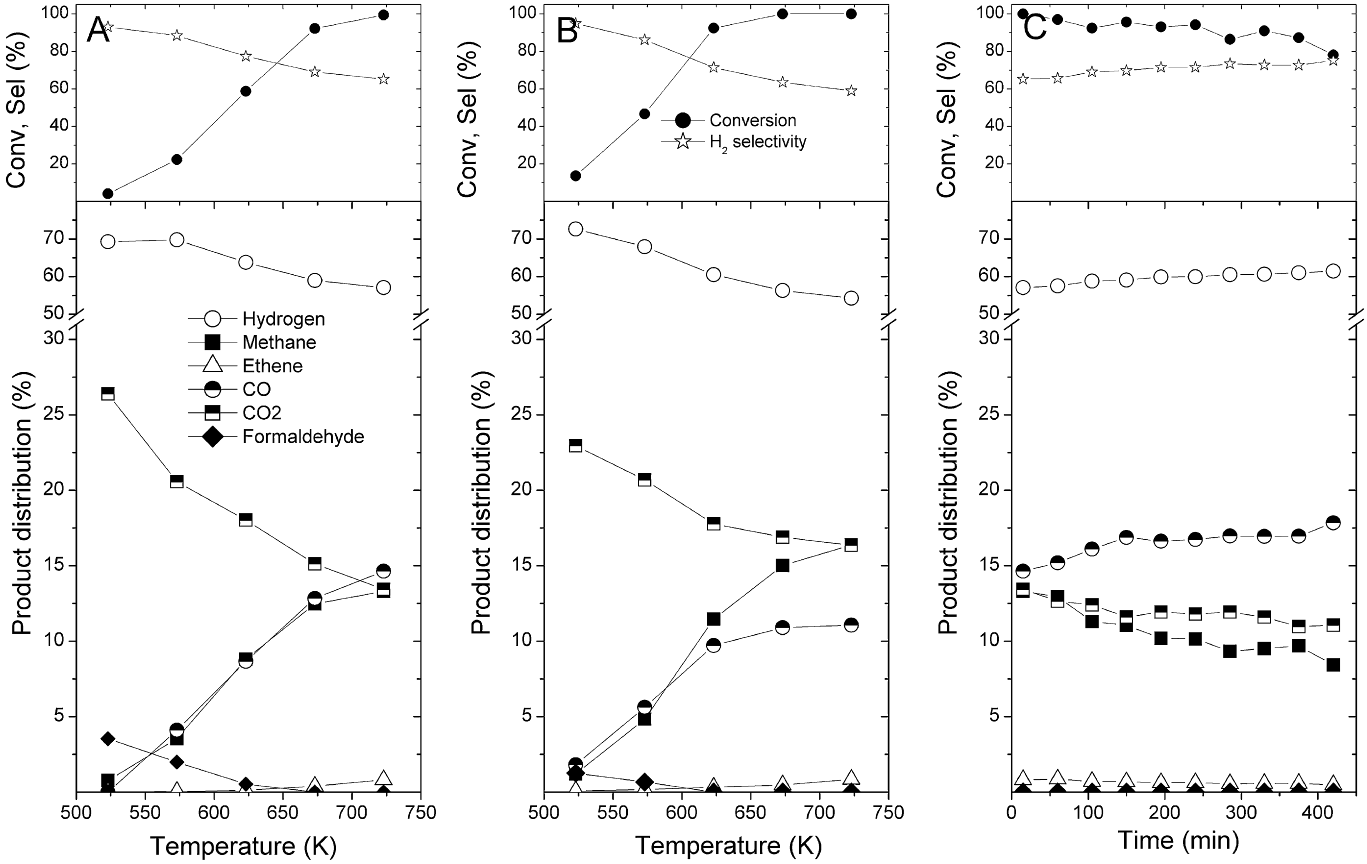

Fig. 9. Effects of water on the product distribution of methanol decomposition on 5% Mo_2C/Norit (A) and 10% Mo_2C/Norit (B) at different temperatures and 5% Mo_2C/Norit in time on stream at 723 K (C).

in terms of H_2 production (Figs. 3C and 9B). Both catalysts exhibited high thermal stability. At 623 K, when only few percent of CO and CO_2 were produced, the 5% Mo_2C/Norit maintained its performance for at least 5 h. At 723 K, when the initial conversion decreased from 100 to 78% in 8 h, the selectivity of H_2 (65–77%) remained practically unaltered, and only slight changes occurred in the distribution of other compounds (Fig. 9C).

4. Discussion

4.1. Main characteristics of Mo_2C formation on carbon

Earlier XRD studies found that Mo_2C is formed in the course of the reduction of MoO_3 on carbon [48,49]. This route represents a new way of preparing highly dispersed Mo_2C. We followed this process using X-ray photoelectron spectroscopy and determining the composition of the gas phase during gradual heating of MoO_3/carbon in H_2 flow [17,18]. The first spectral changes and H_2 consumption were observed at around 573 K. The reaction was terminated at 973 K, when the characteristic binding energies for Mo $3d_{3/2}$–Mo $3d_{5/2}$ of Mo_2C appeared in the XP spectrum. Note that the complete elimination of O 1s was not achieved; a very weak signal at 530.4 eV was always present. The detection of CO and CO_2 above 700 K in the gas phase indicated the occurrence of a direct reaction between partially reduced Mo oxides and carbon. Mo_2C prepared in this way on either carbon Norit or multiwall CNT can be stored after deactivation with 1% oxygen-containing argon and reactivated by reduction at 973 K.

4.2. Interaction of methanol with Mo_2C

Regarding the interaction of methanol with Mo_2C, we can obtain useful hints from previous studies performed under UHV conditions using electron spectroscopy. Ko and Madix [51] reported a marked increase in the stability of methoxy on carbide-modified Mo(100) surface compared with clean Mo(100). Hwo and Chen [50] established that methanol readily dissociates on carbon-modified Mo(100) even at 120 K. They presented spectroscopic evidence for the formation of methoxy species that decomposed completely only above 330 K (Table 1). Methoxy species also were identified on Mo_2C/Mo(100) by high-resolution electron energy loss spectroscopy [52]; similar to Pd(100) [53], alkali additives enhanced its stability.

The formation of methoxy species also has been established on highly dispersed Mo_2C deposited on SiO_2 and on ZSM-5 by FTIR spectroscopy (Table 1). The negative feature in the OH frequency range (Fig. 1) indicates that surface OH groups are consumed in the reaction with methanol to give methoxy species

$$CH_3OH_{(a)} + OH_{(a)} = CH_3O_{(a)} + H_2O_{(g)}. \tag{1}$$

This conclusion is supported by the absorption bands detected (Table 1), particularly by the position of the $\nu_{as}(CH_3)$ and $\nu_s(CH_3)$ vibrations at 2959 and 2859 cm^{-1}, respectively, which are characteristic of adsorbed methoxy [54]. The weaker spectral features at 2934 and 2830 cm^{-1} agree well with the asymmetric and symmetric stretching of adsorbed ethylene formed in the surface interaction (Table 1). Heating the adsorbed layer caused the attenuation of all absorption bands and the appearance of a new peak at 1940 cm^{-1} (not shown), which we attribute to adsorbed CO formed in the decomposition of methoxy species. TPD measurements presented in Fig. 2 show that after the methanol adsorption on Mo_2C/Norit, the irreversibly adsorbed methanol (very likely methoxy species) decomposes to H_2, CO, and CO_2 only above 400 K, with $T_p = 473$–498 K. Very small amounts of methane and ethane also were released. The desorption of methane and hydrogen above 600 and 700 K suggests that a fraction of adsorbed methanol on Mo_2C/Norit was converted into strongly bonded hydrocarbons that decompose only at high temperatures.

4.3. Catalytic decomposition of methanol

Mo_2C formed on carbon Norit and multiwall CNT proved to be a very active catalyst for the decomposition of methanol to yield H_2 and CO,

$$CH_3OH = CO + 2H_2. \tag{2}$$

Complete conversion of the alcohol on 5% Mo_2C/Norit was reached at temperatures as low as 623 K, when the selectivity of H_2 formation exceeded 85%. The detection of formaldehyde at lower temperature and lower Mo_2C content (Fig. 3A) suggests the reaction

$$CH_3OH = HCHO + H_2. \tag{3}$$

As was observed in a separate experiment, Mo_2C catalyzes the decomposition of formaldehyde,

$$HCHO = H_2 + CO, \tag{4}$$

at higher temperatures, which is why it was absent in the reaction products formed on 5% Mo_2C above 573 K (Fig. 3B).

The appearance of methane, particularly at higher Mo_2C loadings (Figs. 3B and 3C) may indicate the reaction

$$CH_3OH_{(a)} = CH_{3(a)} + OH_{(a)} \tag{5}$$

to produce methyl species, which is hydrogenated,

$$CH_{3(a)} + (1/2)H_{2(g)} = CH_{4(g)}, \tag{6}$$

to methane. This reaction pathway has been disputed in the case of Pd(100) surface, for which some spectroscopic evidence has been obtained for the above step [55–60]. In light of this debate, we can counter with the cleavage of the methanolic C–O bond on Mo_2C to some small extent. The active sites for this step could be the carbon-deficient site on the Mo_2C surface, which exhibits high affinity toward oxygen. The reactivity of this site is demonstrated in the promotion of CO dissociation at 300 K [61] as well as the scission of the C–I bond in adsorbed alkyl iodides [62]. The release of strongly bonded O in the form of CO occurred only above ~960 K [60], whereas that of adsorbed I occurred above 1050 K [62].

Another important feature of the Mo_2C on carbon supports is its high thermal stability. This could be its great advantage toward the Cu-based catalyst. No decay in the total conversion and the production of H_2 was experienced at 723 K after 17 h (Fig. 5B). The fact that we measured a relatively high quantity of carbonaceous residue or coke by TPR (Fig. 8) after the reaction suggests that the C-containing compounds formed during the reaction diffused away from the active site of Mo_2C. The carbon support may have a high affinity to accept this kind of carbonaceous species, which exhibited a rather low reactivity. It was hydrogenated only above ~650 K to give a small amount of C_2–C_3 compounds and a large amount of CH_4 above 800 K.

4.4. *Reforming of methanol on Mo_2C/Norit*

As the results show, Mo_2C/Norit also catalyzed the steam reforming of methanol (Fig. 9),

$$CH_3OH + H_2O = 3H_2 + CO_2. \quad (7)$$

This is demonstrated primarily in the changes in product distribution, for example, the increased formation of CO_2 at the expense of CO. We may counter with the water–gas shift reaction,

$$CO_{(g)} + H_2O_{(g)} = CO_{2(g)} + H_{2(g)}, \quad (8)$$

which is well promoted by Mo_2C [63,64]. But this enhanced CO_2 production was accompanied by an increase in H_2 only at lower temperatures 523–623 K (Fig. 9). Above 623 K, the decay in the percentages and selectivities of both H_2 and CO_2 decreased, whereas that of methane and CO increased. From this feature, we may infer the hydrogenation of CO_2,

$$CO_{2(g)} + 4H_{2(g)} = CH_{4(g)} + 2H_2O_{(g)}, \quad (9)$$

which consumes a large amount of H_2.

4.5. *Comparison of the decomposition of methanol and ethanol on Mo_2C*

From the comparison of the catalytic behavior of Mo_2C/C in the decomposition of methanol and ethanol, we can conclude that hydrogen is produced with much higher selectivity and yield from methanol. This is probably because Mo_2C is not active for the cleavage of C–C bond; as a result, it mainly catalyzes the dehydrogenation of ethanol to acetaldehyde and hydrogen. This property of Mo_2C plays an important role in the aromatization of methane [11,12]. Our study of the reaction pathway of CH_2 fragments on Mo_2C/Mo(100) demonstrated its recombination into C_2H_4, the key compound in the aromatization process [65].

5. Conclusions

The findings of the current study can be summarized as follows:

1. Mo_2C prepared on carbon Norit and on multiwall CNT is an effective catalyst for the decomposition of methanol to yield H_2 and CO. Total conversion of methanol can be attained at 623–673 K, with a selectivity for H_2 of $\sim$80%.
2. The catalyst exhibited remarkable stability; the extent of the decomposition of methanol decayed by only a few percent even after 17 h at 723 K.
3. Adding water to the ethanol decreased the amount of CO and increased the selectivity and the yield of H_2 and CO_2 below 623 K.

Acknowledgments

This work was supported by the Hungarian National Office of Research and Technology under contract OMFB-01100/2006. The authors thank Professor I. Kiricsi for the nanotube samples.

References

[1] G. Sandstede, in: T.N. Veziroglu, C. Derive, J. Pottier (Eds.), Proceedings of the Ninth World Hydrogen Energy Conference, Paris, France, 1992, p. 1745.

[2] J.R. Rostrup-Nielsen, in: J.R. Anderson, M. Boudart (Eds.), Catalytic Steam Reforming, in: Catal. Sci. Eng., vol. 5, Springer, Berlin, 1984.

[3] R.A. van Santen, A. de Koster, T. Koerts, Catal. Lett. 7 (1990) 1.

[4] F. Solymosi, Gy. Kutsán, A. Erdőhelyi, Catal. Lett. 11 (1991) 149.

[5] F. Solymosi, A. Erdőhelyi, J. Cserényi, Catal. Lett. 16 (1992) 399.

[6] M. Belgued, H. Amariglio, P. Pareja, A. Amariglio, J. Sain-Just, Catal. Today 13 (1992) 437.

[7] F. Solymosi, A. Erdőhelyi, J. Cserényi, J. Catal. 147 (1994) 272.

[8] F. Solymosi, J. Cserényi, Catal. Today 21 (1994) 561.

[9] V.R. Choudhary, V. Nayak, Zeolites 5 (1985) 325.

[10] T.V. Choudhary, E. Aksoylu, D.W. Goodman, Catal. Rev. Sci. Eng. 45 (2003) 151.

[11] F. Solymosi, J. Cserényi, A. Szőke, T. Bánsági, A. Oszkó, J. Catal. 165 (1997) 150.

[12] D.W. Wang, J.H. Lunsford, M.P. Rosynek, J. Catal. 169 (1997) 347.

[13] A. Széchenyi, F. Solymosi, Appl. Catal. A Gen. 306 (2006) 149, and references therein.

[14] A. Széchenyi, R. Barthos, F. Solymosi, Catal. Lett. 110 (2006) 85.

[15] A. Széchenyi, R. Barthos, F. Solymosi, J. Phys. Chem. B 110 (2006) 21816.

[16] R. Barthos, A. Széchenyi, F. Solymosi, J. Catal. 247 (2007) 368.

[17] R. Barthos, A. Széchenyi, F. Solymosi, Catal. Lett., in press.

[18] R. Barthos, A. Széchenyi, Á. Koós, F. Solymosi, Appl. Catal. A Gen. (2007), doi:10.1016/j.apcata.2007.03.040, in press.

[19] J. Patt, D.J. Moon, C. Phillips, L.T. Thompson, Catal. Lett. 65 (2000) 193.

[20] K. Oshikawa, M. Nagai, S. Omi, Jpn. J. Appl. Phys. 39 (2000) 4456.

[21] N. Iwasa, S. Kudo, H. Takahashi, S. Masuda, N. Takezawa, Catal. Lett. 19 (1993) 211.

[22] N. Iwasa, S. Masuda, N. Ogawa, N. Takezawa, Appl. Catal. A 125 (1995) 145.

[23] N. Takezawa, N. Iwasa, Catal. Today 36 (1997) 45.

[24] J.P. Breen, J.R.H. Ross, Catal. Today 51 (1999) 521.

[25] J.P. Breen, F.C. Meunier, J.R.H. Ross, Chem. Commun. (1999) 2247.

[26] S. Velu, K. Suzuki, M. Okazaki, M.P. Kapoor, T. Osaki, F. Ohashi, J. Catal. 194 (2000) 373.

[27] N. Iwasa, T. Mayanagi, S. Masuda, N. Takezawa, React. Kinet. Catal. Lett. 69 (2000) 355.

[28] Y.H. Chin, R. Dagle, J. Hu, A.C. Dohnalkova, Y. Wang, Catal. Today 77 (2002) 79.

[29] S.T. Liu, K. Takahashi, M. Ayabe, Catal. Today 87 (2003) 247.

[30] N. Iwasa, N. Takezawa, Top. Catal. 22 (2003) 215.

[31] Z. Chen, K.M. Neyman, A.B. Gordienko, N. Rosch, Phys. Rev. B 68 (2003) 075417.

[32] X.R. Zhang, P. Shi, J. Zhao, M. Zhao, C. Liu, Fuel Process. Technol. 83 (2003) 183.

[33] J. Agrell, H. Birgersson, M. Boutonnoet, I. Melian-Cabrera, R.M. Navarro, J.L.G. Fierro, J. Catal. 219 (2003) 389.

[34] Y.H. Chin, Y. Wang, R.A. Dagle, X.H.S. Li, Fuel Process. Technol. 83 (2003) 193.

[35] S.T. Liu, K. Takahashi, K. Uematsu, M. Ayahe, Appl. Catal. A Gen. 277 (2004) 265.

[36] P.H. Matter, D.J. Braden, U.S. Ozkan, J. Catal. 223 (2004) 340.

[37] T. Shishido, Y. Yamamoto, H. Morioka, K. Takaki, K. Takehira, Appl. Catal. A Gen. 263 (2004) 249.

[38] G. Jacobs, P.M. Patterson, U.M. Graham, A.C. Crawford, A. Dozier, B.H. Davis, J. Catal. 235 (2005) 79.

[39] S.T. Liu, K. Takahashi, K. Uematsu, M. Ayahe, Appl. Catal. A Gen. 283 (2005) 125.

[40] A. Mastalir, B. Frank, A. Szizybalski, H. Soerijanto, A. Deshpande, M. Niederberger, R. Schomacker, R. Schlogl, T. Ressler, J. Catal. 230 (2005) 464.

[41] P.H. Matter, U.S. Ozkan, J. Catal. 234 (2005) 463.

[42] H. Oguchi, T. Nishiguchi, T. Matsumoto, H. Kanai, K. Utani, Y. Matsumura, S. Imamura, Appl. Catal. A Gen. 281 (2005) 69.

[43] E.S. Ranganathan, S.K. Bej, L.T. Thompson, Appl. Catal. A Gen. 289 (2005) 153.

[44] S.T. Liu, K. Takahashi, K. Fuchigami, K. Uematsu, Appl. Catal. A Gen. 299 (2006) 58.

[45] M. Lenarda, E. Moretti, L. Storaro, P. Patrono, F. Pinzari, E. Rodrígez-Castellón, A. Jiménez-López, G. Busca, E. Finocchio, T. Montanari, R. Frattini, Appl. Catal. A Gen. 312 (2006) 220.

[46] S.S.-Y. Lin, W.J. Thomson, T.J. Hagensen, S.Y. Ha, Appl. Catal. A Gen. 318 (2007) 121.

[47] A. Kukovecz, T. Kanyo, Z. Konya, I. Kiricsi, Carbon 43 (2005) 994.

[48] D. Mordenti, D. Brodzkí, G. Djega-Mariadassou, J. Solid State Chem. 141 (1998) 114.

[49] C. Liang, Z. Wei, C. Li, Stud. Surf. Sci. Catal. 143 (2002) 975, and references therein.

[50] H.H. Hwo, J.G. Chen, Surf. Sci. 536 (2003) 75.

[51] E.I. Ko, R.J. Madix, Surf. Sci. 112 (1981) 373.

[52] A. Farkas, Ph.D. thesis, University of Szeged, 2007.

[53] F. Solymosi, A. Berkó, Z. Tóth, Surf. Sci. 285 (1993) 197.

[54] N. Takezawa, H. Kobayashi, J. Catal. 25 (1972) 179.

[55] R.J. Levis, J. Zhicheng, N. Winograd, J. Am. Chem. Soc. 111 (1989) 4605.

[56] X. Guo, L. Hanley, J.T. Yates Jr., J. Am. Chem. Soc. 111 (1989) 3155.

[57] F. Solymosi, K. Révész, J. Am. Chem. Soc. 113 (1991) 9145.

[58] M. Rebholz, N. Kruse, J. Chem. Phys. 95 (1991) 7745.

[59] J.-J. Chen, Z.-C. Jiang, Y. Zhou, B.R. Chakraborty, N. Winograd, Surf. Sci. 328 (1995) 248.

[60] M. Morkel, V.V. Kaichev, G. Rupprechter, H.-J. Freund, I.P. Prosvirin, V.I. Bukhtiyarov, J. Phys. Chem. B 108 (2004) 12955.

[61] F. Solymosi, L. Bugyi, A. Oszkó, Catal. Lett. 57 (1999) 103.

[62] A.P. Farkas, Á. Koós, L. Bugyi, F. Solymosi, Surf. Sci. 600 (2006) 2355.

[63] J. Patt, D.J. Moon, C. Phillips, L.T. Thompson, Catal. Lett. 65 (2000) 193.

[64] K. Oshikawa, M. Nagai, S. Omi, Jpn. J. Appl. Phys. 39 (2000) 4456.

[65] F. Solymosi, L. Bugyi, A. Oszkó, I. Horvath, J. Catal. 185 (1999) 160.